The influence of chemical environment on the infrared spectra of embedded molecules in astrophysical ices

Victor S. Bonfim[1] and Sergio Pilling[1,2]

[1]Instituto de Pesquisa e Desenvolvimento, Universidade do Vale do Paraíba - UNIVAP,
Av. Shishima Hifumi, 2911, Urbanova, São José dos Campos, SP - Brazil
email: victordsb@gmail.com

[2]Instituto Tecnológico de Aeronáutica, ITA - DCTA
Praça Marechal Eduardo Gomes, 50 - Vila das Acacias, São José dos Campos, SP - Brazil
email: sergiopilling@yahoo.com.br

Abstract. In this work, one intends to computationally simulate and investigate, via thermochemical calculations, how the chemical environment influences some molecular properties, such as IR spectra and absorption cross section, of individual species embedded in the solid phase employing the Polarized Continuum Model (PCM) approach. The trial molecules used here to check these effects are CO, CO_2 and H_2O. The solid phase (bulk ice) is simulated using different dielectric constant values representing different types of astrophysical ice at PCM approach. The effect of temperature is also investigated since it is known it affects the dielectric constant of the solvent medium.

Keywords. ISM: molecules, abundances, infrared: general, dense matter, astrochemistry

1. Introduction

Both on Earths surface and in astrophysical environments, various molecules are found embedded into solid water structure. In the case of interstellar medium, the astrophysical ice mantles over dust grains surface can vastly vary in composition. For some cases, the chemical species of interest are extremely diluted in the icy matrix containing them. Besides solid water, the main constituents of such matrices are also CO_2, CO, CH_3OH, or CH_4, among others, and a combination of them.

Astrophysical ices may also vary a lot in temperature, depending on various parameters of the surrounding environment. Nonetheless, they can be divided (at least) in two temperature regimes for the ice mantles (Van Dishoeck *et al.* 2013), and these regimes we call in the present study as cold ice and hot ice. This arbitrary classification is illustrated in Figure 1. for an astrophysical context where there is ice at both cold and hot regimes, depicted in the same figure in blue and in red colors, respectively.

As a first approximation, the net effect of the solvent medium (solid matrix) in a given chemical species which is there embedded can be accounted by simply considering the presence of an average electric field surrounding this species, this field being parameterized by the dielectric constant (ε) of the medium. This level of description can be achieved employing Polarized Continuum Model (PCM) approach (Miertuš *et al.* 1981), which is implemented in several computational Quantum Chemistry packages. Indeed, there are already some works in literature where the authors utilized PCM (or a similar continuum solvent model) to model the average icy matrix effect on the embedded molecule reactivity (Bonfim *et al.* 2015, 2017; Park & Woon 2004; Pilling *et al.* 2011a; Woon & Park 2004). However, none of them attempted to simulate the effects of one

Figure 1. Representative illustration of an astrophysical scenario where ice is present at two regimes of temperature, here called cold ice (in blue) and hot ice (in red), comprising a star formation region in the Eagle Nebula (adapted from Constellation Guide 2013).

specific bulk ice property on the vibrational modes of each trapped molecule, which are closely related to the determination of molecular abundances in observational studies.

In this work we evaluate, through vibrational analysis from PCM ab initio calculations, how the chemical environment influences some features of molecular infrared (IR) spectrum profiles, specifically, the peak positions and their respective intensities, of three trial molecules. The chosen molecules are CO, CO_2 and H_2O, thus involving two polar molecules and one nonpolar species (CO_2). Very often these three molecules are the major components of the astrophysical ices matrix, from which H_2O is the dominant one for most cases. Very often these three molecules are the major components of the astrophysical ices matrix, from which H2O is the dominant one for most cases. Accordingly, we also intend to probe the role of the studied properties in determining molecular abundances.

2. Methods and Models

All Calculations were performed at Second-order Møller-Plesset perturbation theory (MP2) level, with the correlation consistent triple zeta basis set, or just cc-pVTZ (Dunning Jr 1989). The number of electrons in the system varies quite well among the molecules investigated here, and also for a larger set of molecules on which calculations are in progress. Thus, for reasons of computational convenience, we have used the MP2/cc-pVTZ calculation level for all the electronic structure calculations of the current work. The chemical species had the equilibrium geometry confirmed for each ε value by applying harmonic vibrational analysis, which has also provided the desired output data. The complete study was performed using the Gaussian 09 package (Frisch *et al.* 2010).

An interesting feature of vibrational intensity I changing is to allow one to know the influence felt by band strength B, since the ratio I/I_0 is equivalent to the quotient B/B_0. This latter one is a molecular property (rigorously, it varies with each vibrational mode) of major astrophysical interest as it is sensitive to changes in the chemical environment. This relationship between I and B can be seen from the equation:

$$B = \frac{2.3}{N}A, \ A \propto I \ [cm\ molecule^{-1}] \tag{2.1}$$
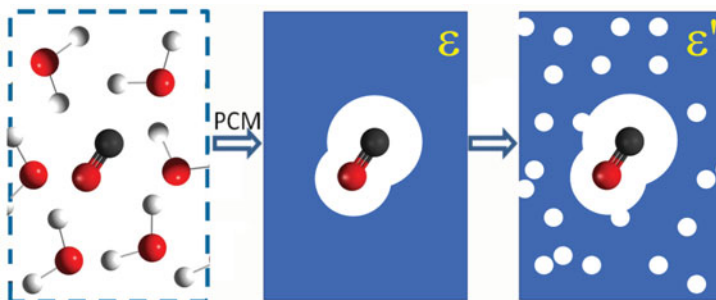
Figure 2. Illustration of the PCM approximation and the porous sample approximation (solid filled with holes containing vacuum). The molecular environment is represented by its dielectric constant ε and here ε' stands for the dielectric constant of the porous sample ($\varepsilon' < \varepsilon$). See details in the text.

where N is the column density of a given species, and A is the band area (in units of cm^{-1}) of a specific IR vibrational mode. From this equation (see e.g. Pilling *et al.* 2011b), we note that when comparing two samples containing the same N, variations in the ratio between two B values, namely B and B_0, will be equivalent to the ratio between I and I_0, assuming the change in A is very little affected by enlargement or narrowing of the peak. Once we are aware that our theory level is not accurate enough to predict each I value quantitatively, predicting the ratio of two band strengths gets us as close as possible from connections with observational and / or experimental data. Due to the exposed equivalence, Intensity variations are expressed in this work as B/B_0.

In the adopted effective-medium approach context, we can use the link between ε and other physicochemical properties of the bulk ice to probe how they influence the IR spectra of the embedded molecules. For practical means, it may be assumed that variations in such properties, such as ice temperature, are dominated by changes in the solid water matrix, and consequently in the corresponding ε values. In the current study, we propose an exponential function to fit ε as a function of temperature T, since ε (T) for $H_2O(s)$ may vary quite abruptly in the studied interval of 10-140 K (Tsekouras *et al.* 1998). The employed function is presented as follows:

$$\varepsilon = (9.0 \times 10^{-6}) \, e^{0.12\,T} + 3.0 \qquad (2.2)$$

Aiming not to get too far from experimental data, we have constrained the function during fitting process in order to reproduce ε (10 K) $\sim$ 3 and ε (140 K) = 180 (Johari & Whalley 1981; Tsekouras *et al.* 1998). Concerning porosity, an increase in the ice porosity can be simulated by decreasing the ice ε_{pi}, starting from the ε value for the compact ice, and adopting the proper relation between the two simulated quantities. Some variety of such relations have already been proposed and described in literature, and here we adapt the model from Sun & Goldberg (2005) for ternary mixtures:

$$Porosity = 100\% \times \frac{\sqrt{\varepsilon_{pi}} - \sqrt{\varepsilon}}{\sqrt{\varepsilon_{pi}} - 1} \qquad (2.3)$$

In 2.3, ε_{pi} is the dielectric constant for the pure ice, assuming a structure without pores. In this work we have considered two temperature regimes, cold ices (close to 10 K) (Tsekouras et al., 1998), and hot ices, where ε_{pi} reaches about 180 for 140 K (Aragones et al., 2011; Johari & Whalley, 1981). A schematic illustration of the PCM approximation and how it approaches a porous ice is shown in Figure 2, in which the white circles represent holes containing vacuum ($\varepsilon = 1$).
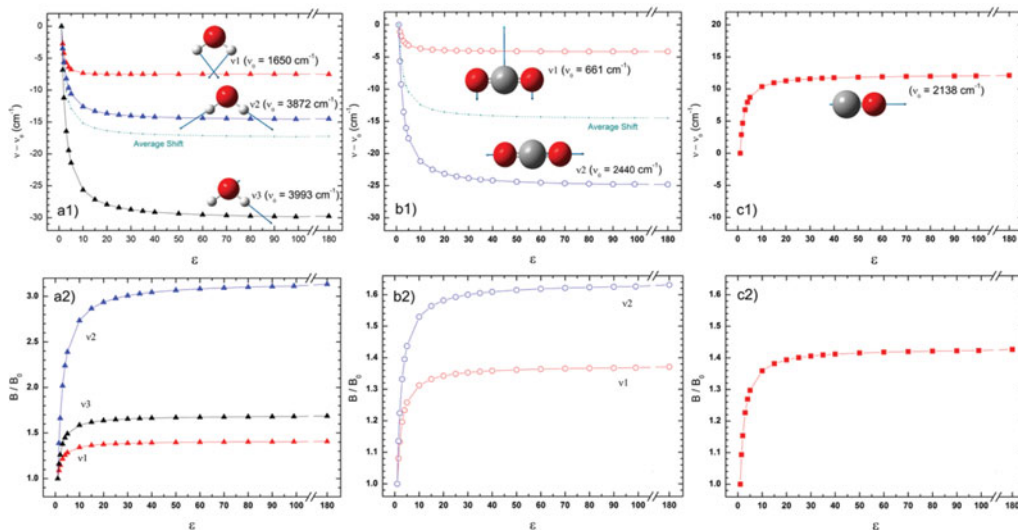
Figure 3. Changes in the IR spectral features of each vibrational mode of H_2O, CO_2 and CO molecules embedded in the icy matrix as a function of its ε, displayed in two different aspects: 1) frequency shifts; 2) band strength ratios. Results from vacuum calculations ($\varepsilon = 1$) are considered as reference values and are indicated by ν_0 and B_0 symbols. See details in the text.

3. Results and Discussion

The evaluated IR spectrum features have presented considerable variations with systematic ε changing. Figure 3 shows those variations for the three studied molecules, H_2O, CO_2 and CO in the panels a, b and c, respectively. The increase or decrease in the vibrational frequencies (in wavenumbers) is displayed in panels numbered as "1" and panels numbered as "2" show the variations on band strengths. In each case, the subscript "0" refers to the value obtained for the vacuum environment, where $\varepsilon = 1$ (by definition).

Regarding wavenumbers, the general trend was a decrease with ε increasing, indicating there would be a shift of the peaks to the right in their IR spectrum, which would also be worth if we expressed the results in wavelengths. The only exception to this trend was the CO vibrational mode, which in a spectrum would have shifted to the left. The maximum wavenumber shift occurred for the asymmetric stretch of the water molecule. This species also has the largest average shift, although the highest variation on CO_2 vibrational modes (also for an asymmetric stretch) is greater than the average shift for H_2O.

Differently from frequencies, band strengths have all varied in the same way for the investigated molecules, rapidly increasing with ε for the $1 < \varepsilon < 15$ interval, and showing a gradually slow increase for roughly $\varepsilon = 15$ onwards. Interestingly, the lowest-frequency modes all had a similar increase in magnitude, while the CO_2 asymmetric stretching (asym. str.) mode increased twice that amount. In turn, the water mode with highest B/B_0 values, the symmetric stretching mode, showed a maximum growing of around three times the original value, or about four times the maximum increase in B/B_0 for the CO_2 asym. str. mode. Hence, our results bring evidence that not taking in account at least the average effects of the chemical environment can lead to significant errors in molecular abundance determinations.

Figure 4 shows the total set of probable effects of changing ice temperature or ice porosity in the IR spectra for all the studied molecules. Here, these changes are presented
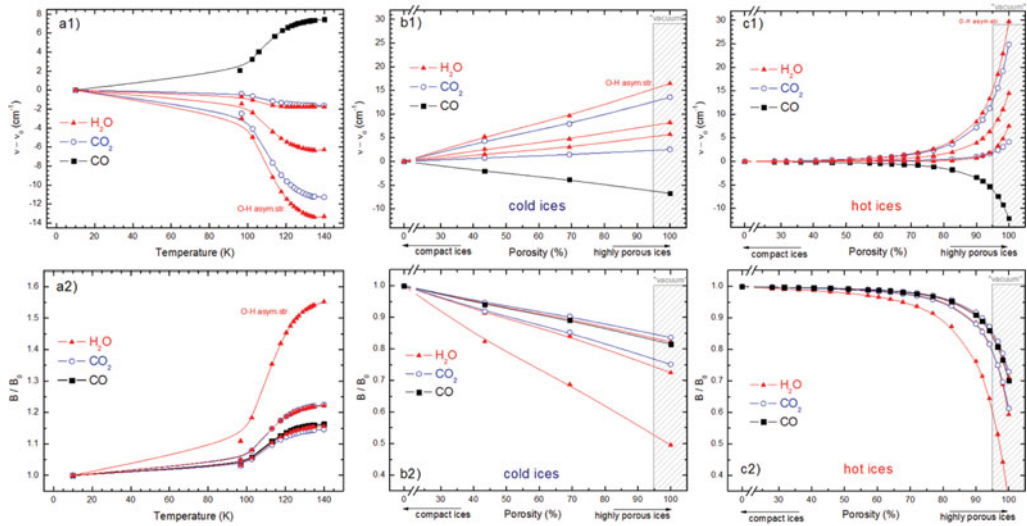
Figure 4. Changes in the IR spectral features of all studied species H_2O, CO_2 and CO embedded in a typical water icy matrix, as a function of temperature - from 10 K up to 140 K - (a) and porosity for both cold ice (b) and hot ice (c). Frequency shifts (ν - ν_0) and band strength ratios (B/B_0) are presented in top (1) and bottom (2) panels, respectively (ν_0 and B_0 are equivalent to the results for $\varepsilon = 3$, except for hot ice panels, where it was considered $\varepsilon_{pi} = 180$). The shaded area assumes that porosity above 95% would not allow an ice phase to exist.

as a function of temperature (from 10 K up) and porosity for both cold ice and hot ice. Here, the subscript "0" denotes $\varepsilon = 3$ results when probing temperature effects, and concerning results about porosity effects, it implies the ν_0 and I values obtained for ε_{pi}. Still related to porosity investigations, there are shaded areas in the corresponding panels, highlighting that a value equal to or very close to 100% would imply in the absence of a solid matrix. Nevertheless, we decided to keep these points in view in order to assist in visualizing the identified tendencies in vibrational frequencies and band strengths. Strictly saying, all the data displayed in this figure comes from the same calculation results already presented in Figure 3, but here the presentation format has changed to fit the evaluated properties.

The observed variations profile for both wavenumbers and band strength ratios are quite dependent from the relationship between ε and the linked property. For temperature, they are biased from the mathematical limitation in getting the inverse function of 2.2, which is a natural logarithm, and consequently is not defined for $\varepsilon = 3$ or lower. Also, the investigated vibrational modes have shown to be much more sensitive to the ice porosity while incorporated into cold ices, than into hot ices. Evidently, this comparison disregards data related to extremely high porosity (close to 95% and above). A recurring overall trend is that the "$\nu1$" mode (lowest frequency) of each molecule has shown to be the least sensitive to variations in the surrounding chemical environment.

It is important to keep in mind that our vibrational modes analysis is based on an average field approach, which hinders direct comparisons with laboratory spectra. Even so, the qualitative relevance of the predicted deviations for astrophysical scenarios still remains. Especially in the case of amorphous ices, usually formed at low temperatures, which have been subject of Astrochemistry studies (Collings *et al.* 2004; Öberg *et al.* 2009; Pilling & Bergantini 2015).

4. Conclusions

For most vibrational modes employed in this study, band strengths have increased with ε, which implies they have decreased with respect to porosity. The frequency shifts (in cm^{-1}) showed opposite behavior in relation to the band strengths, with the exception of the CO mode, revealing that different vibrational modes are influenced by the solid matrix diversely. In order to achieve a more precise description of this influence, a larger set of molecules would be desirable. Besides that, all the trends here observed seem to be more pronounced in low temperature ices than in higher temperature ones.

The B/B_0 value for the H_2O symmetric stretching mode varied by more than 50% with the change from $\varepsilon = 3.0$ to $\varepsilon = 180$, which represents the difference in our models from a cold astrophysical ice to a hot ice. The determination of molecular abundances depends a lot on the band strength. Therefore, it becomes clear that direct transposition of a B value obtained in one experiment (or observation) to another with different physicochemical characteristics can lead to considerable errors in abundance determinations.

This study may also provide a better understanding of some astrophysical ices properties and their interaction with radiation. Based on the IR spectral profile of diluted species, one could be able to infer physical and chemical properties of the surrounding medium.

References

Aragones, J. L., MacDowell, L. G., & Vega, C. 2011, *J. Phys. Chem. A* 115, 5745-5758

Bonfim, V. S., Castilho, R. B., Baptista, L., & Pilling, S. 2017, *Phys. Chem. Chem. Phys.* submitted

Bonfim, V. S., Castilho, R. B., Baptista, L., & Pilling, S. 2015 *J. Phys. Conf. Ser.* 635, 102012. doi:10.1088/1742-6596/635/10/102012

Collings, M. P., Anderson, M. A., Chen, R., Dever, J. W., Viti, S., Williams, D. A., & McCoustra, M. R. S. 2004 *Mon. Not. R. Astron. Soc.* 354, 1133-1140

Dunning Jr, T. H. 1989, *J. Chem. Phys.* 90, 1007

Frisch, M. J., Trucks, G. W., Schlegel, H. B., Scuseria, G. E., Robb, M. A., Cheeseman, J. R., Scalmani, G., Barone, V., Mennucci, B., Petersson, G. A., Nakatsuji, H., Caricato, M., Li, X., Hratchian, H. P., Izmaylov, A. F., Bloino, J., Zheng, G., Sonnenberg, J. L., Hada, M., Ehara, M., Toyota, K., Fukuda, R., Hasegawa, J., Ishida, M., Nakajima, T., Honda, Y., Kitao, O., Nakai, H., Vreven, T., Montgomery Jr., J. A., Peralta, J. E., Ogliaro, F., Bearpark, M., Heyd, J. J., Brothers, E., Kudin, K. N., Staroverov, V. N., Kobayashi, R., Normand, J., Raghavachari, K., Rendell, A., Burant, J. C., Iyengar, S. S., Tomasi, J., Cossi, M., Rega, N., Millam, J. M., Klene, M., Knox, J. E., Cross, J. B., Bakken, V., Adamo, C., Jaramillo, J., Gomperts, R., Stratmann, R. E., Yazyev, O., Austin, A. J., Cammi, R., Pomelli, C., Ochterski, J. W., Martin, R. L., Morokuma, K., Zakrzewski, V. G., Voth, G. A., Salvador, P., Dannenberg, J. J., Dapprich, S., Daniels, A. D., Farkas, O., Foresman, J. B., Ortiz, J. V, Cioslowski, J., & Fox, D. J. 2010, Gaussian 09, Revision B.01

Constellation Guide 2013, Eagle Nebula - Messier 16 URL: http://www.constellation-guide.com/eagle-nebula-messier-16/ (accessed 4.2.17)

Johari, G. P., & Whalley, E. 1981, K. *J. Chem. Phys.* 75, 1333-1340

Miertuš, S., Scrocco, E., & Tomasi, J. 1981, *Chem. Phys.* 55, 117-129

Öberg, K. I., Linnartz, H., Visser, R., & van Dishoeck, E. F. 2009, *ApJ* 693, 1209-1218

Park, J. Y., & Woon, D. E. 2004, *J. Phys. Chem. A.* 108, 6589-6598

Pilling, S., Baptista, L., Boechat-Roberty, H. M., & Andrade, D. P. P. 2011a, *Astrobiology* 11, 883-893

Pilling, S. & Bergantini, A. 2015, *ApJ* 811, 151

Pilling, S., Duarte, E. S., Domaracka, A., Rothard, H., Boduch, P., & Silveira, E. F. Da 2011b *Phys. Chem. Chem. Phys.* 13, 15755-15765

Sun, Y. F., & Goldberg, D. 2005, *Geophys. Res. Lett.* 32, L04313

Tsekouras, A. A., Iedema, M. J., & Cowin, J. P. 1998, *Phys. Rev. Lett.* 80, 5798-5801

Van Dishoeck, E. F., Herbst, E., & Neufeld, D. A. 2013, *Chem. Rev.* 113, 9043-9085

Woon, D. E., & Park, J. 2004, *ApJ. J.* 607, 342-345